Research Article | Vol. 31, No. 19 / 11 Sep 2023 / Optics Express 31644
Optics EXPRESS

Investigation of perfect narrow-band absorber in silicon nano hole array

QIANG LI,[1,2,3,*] HAOLONG TANG,[1,2] YI ZHAO,[1,2] HAI LIU,[1,2] ZHENFENG SHEN,[1,2] TONGTONG WANG,[1,2] HAIGUI YANG,[1,2] XIAOYI WANG,[1,2] YAN GONG,[3,4] AND JINSONG GAO[1,2,3,5]

[1]*Changchun Institute of Optics, Fine Mechanics and Physics, Chinese Academy of Sciences, Changchun 130033, China*
[2]*Key Laboratory of Optical System Advanced Manufacturing Technology, Chinese Academy of Sciences, Changchun 130033, China*
[3]*University of Chinese Academy of Sciences, Beijing 100039, China*
[4]*Jiangsu Key Laboratory of Medical Optics, Suzhou Institute of Biomedical Engineering and Technology, Chinese Academy of Sciences, Suzhou 215163, China*
[5]*Jilin Provincial Key Laboratory of Advanced Optoelectronic Equipment and Instrument Manufacturing Technology, Changchun 130033, China*
[*]*liqiang@ciomp.ac.cn*

Abstract: In this paper, we proposed a triple layer structure consisting of the bottom silver layer, thin silicon oxide space layer, and ultrathin semiconductor silicon film with nano hole array achieving three absorption peaks with narrow band. The absorption spectrum can be easily controlled by adjusting the structural parameters including the radius and period of the nano hole array, and the maximal absorption can reach 99.0% and the narrowest full width of half maximum can reach about 6.5 nm in theory. We also clarified the physical mechanism of the proposed structure in details by finite-difference time-domain simulation, in which the three narrow band perfect adsorption peaks can be attributed to electric dipole resonance, magnetic dipole resonance and plasmonic resonance respectively. At the same time, we used a low-cost nanosphere lithography method to fabricate the proposed nano hole array in large area. In experiment, the absorption peak of the proposed triple layer structure can reach up to 98.3% and the narrowest full width of half maximum can reach up to about 10.1 nm. The highest quality factor Q can reach up to 98.4. This work can open a new avenue for high-quality factor narrow band perfect absorption using ultrathin semiconductor film and benefit for many fields such as infrared sensors, plasmonic filters, and hyperspectral imaging.

1. Introduction

Perfect absorption in an ultrathin layer of deeply subwavelength thickness is always a challenge for both fundamental theory and practical applications such as energy harvesting [1–5], sensing [6–12], photodetectors [13–15], surface-enhanced Raman scattering (SERS) [16–18], and plasmonic photocatalysts [19–21]. Perfect absorption within an ultrathin layer can be achieved by subwavelength structures creating a critically coupled resonance, which usually involves noble metal such as gold (Au) and silver (Ag). These micro or nano structures can couple the incident light into either propagating surface plasmon polariton (SPP) at the interface of the metal and dielectric, or a localized surface plasmons (LSPs) around the metal structures [22–33]. Perfect absorption based on the subwavelength structures have been studied widely in the arrays of metallic gratings, nano cube, nanoparticles, and nano hole recently due to the controllable optical properties by engineering the shape, size, material of the structure as well as their dielectric environment. However, the fabrication of these subwavelength structures is a challenge because the tiny size. In addition, the use of the metal will bring in large Ohmic loss, which makes it

#501458 https://doi.org/10.1364/OE.501458
Journal © 2023 Received 24 Jul 2023; revised 28 Aug 2023; accepted 30 Aug 2023; published 8 Sep 2023

Optics EXPRESS

incompatible with the standard optoelectronic applications because the photocurrent should be extracted. What is worse, these nano structures made up with metals usually have the full width of half maximum (FWHM) much larger than dozens of nanometers, which severely limited its application in narrow band perfect absorber.

Semiconductor materials such as silicon (Si) and germanium (Ge) are promising and widely used in solar cell, photo-detection, and energy harvest because they have the advantages of high performance, low cost, and compatible with the standard optoelectronic fabrication. However, achieving perfect absorption in ultrathin semiconductor layer is always a critical and long-standing challenge. In recent years, Capasso et al. proposed a simple thin film structure consisting of a golden reflective mirror and an ultrathin semiconductor Ge layer with thickness of about 20 nanometers [34]. This kind of ultrathin lossy semiconductor film is different from traditional optical coatings because the imaginary part of the complex refractive index has an important impact on the phase change at the interface, which can form a dip in the measured reflection spectrum due to the strong Fabry–Perot (FP) type interference effect. Such a simple architecture has a strong light trapping ability in ultrathin thin film and has great potential to boost the performance of photodetection, photovoltaics, solar cells, and optical filters. Since then, many excellent studies have achieved perfect absorption using ultrathin lossy semiconductor materials [35–41]. These works usually focus on the broadband perfect absorption. In recent years, some works also studied the absorption with narrow band [42–46]. However, most of them stayed in theoretical simulation without any experiment. Achieving high-quality factor narrow band perfect absorption with high refractive index and low optical loss materials have important research significance, which should be demonstrated as soon as possible.

In this paper, we investigate a triple layer metal-dielectric-dielectric structure consisting of the metal plane, thin space layer, and ultrathin semiconductor film with nano hole array. Using this structure, perfect absorption with three narrow band can be achieve in the near infrared region. The peak and FWHM in the absorption spectrum are nearly 100% and 6.5 nm respectively obtained from simulation. In the meantime, a comprehensive analysis of physical mechanism is demonstrated, in which magnetic resonance, electric resonance and plasmonic resonance supported by the nano hole array play an important role. And then, we use a low-cost nanosphere lithography method to fabricate the proposed nano hole array in large area, which proves the simulation results. This work can open a new avenue for narrow band perfect absorption using ultrathin semiconductor film and benefit for many fields such as infrared sensors, plasmonic filters, and hyperspectral imaging.

2. Model and simulation methods

The proposed triple layer metal-dielectric-dielectric structure is shown in Fig. 1(a). The material of the bottom metal layer is silver (Ag) with 100 nm thickness, which is thick enough so that no incident light can pass through the structure. A nano hole array in a hexagonal lattice is patterned on the top ultrathin silicon (Si) layer as shown in Fig. 1. At the same time, a thin silicon oxide (SiO_2) layer is spaced between the Ag mirror and Si layer. The period and diameter of the nano hole are L and $2r$. The thickness of the middle SiO_2 layer and ultrathin Si layer are d_2 and d_1. In order to investigate the optical characteristic of the proposed structure, the 3D finite-difference time-domain (FDTD) method with a commercial software (Lumerical, FDTD solutions) is performed where the perfectly matched layers (PML) are applied in the z axis and periodic boundary conditions are used for a unit cell in the x-y plane. A discrete mesh with size of 2 nm × 2 nm × 1 nm is set in the simulation region for the absolute convergence. The permittivity of Ag, SiO_2, and Si used in FDTD simulation are extracted from the data of Palik [47] as the Fig. 1(b) shown. The incident light with a wavelength range from 800 nm to 1200 nm propagates along the negative z direction with the E field polarization in the x direction. The absorption spectrum is $A = 1\text{-}R$ where R is the reflection obtained from the reflection monitor.

Optics EXPRESS

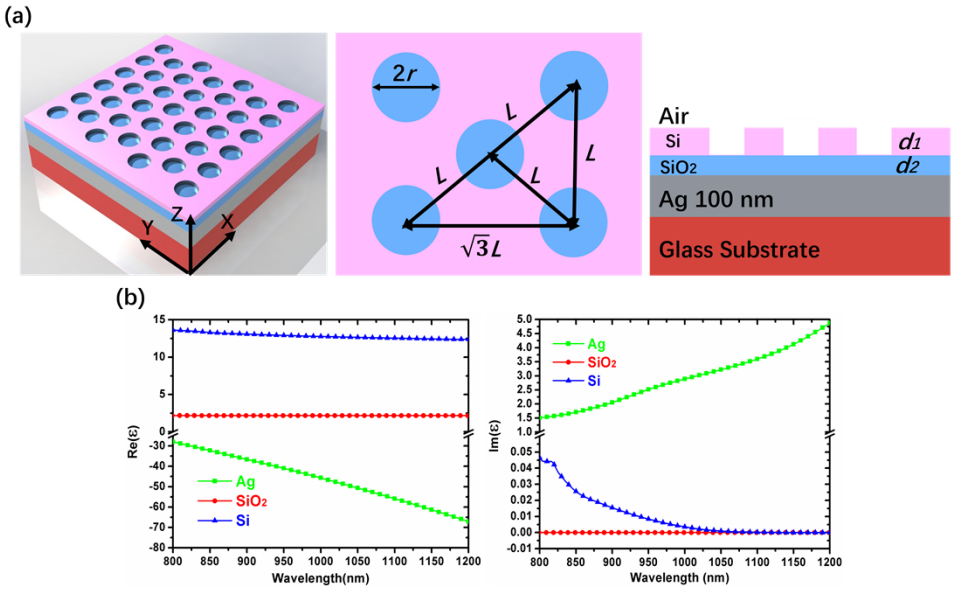

Fig. 1. (a) Schematic of the triple-layer structure. Top and cross-sectional view of the structure. (b) The permittivity of Ag, SiO_2, and Si extracted from the data of Palik.

3. Numerical investigation and theory analysis

First of all, the proposed triple layer structure with nano hole array patterned on the top ultrathin Si layer is investigated. The radius r of the nano hole is swept using FDTD simulation with fixed period L (700 nm). The thickness of the SiO_2 and Si layers are 50 nm and 100 nm respectively. The simulated absorption as a function of r and incident wavelength is shown in Fig. 2(a). As we can see, three different electromagnetic modes lead to three distinct absorption peaks indicated by A_1, A_2 and A_3, whose location depend on the radius. The absorption band is narrow and the absorption is high. Figure 2(b) shows three different radius ($r = 140$ nm,160 nm and 180 nm) of the nano hole marked by the red, green and blue lines with the fixed period $L = 700$ nm. In the meanwhile, we also sweep the period L with the fixed radius r (160 nm). The simulated result is shown in Fig. 2(c), in which three absorption peaks strongly depend on the period L. While for the Fig. 2(d) shows the absorption when the period L is different (650 nm, 700 nm and 750 nm) with the fixed radius r 160 nm. From Fig. 2(b) and Fig. 2(d) we can see the bands of absorption spectrum varies from a few nanometers to around ten nanometers. For example, when the period and radius of the nano hole array are 700 nm and 160 nm, the green line in Fig. 2(b), it is evident that three absorption peaks appear at the wavelengths of 864.0 nm, 985.0 nm and 1102.0 nm with a narrow FWHM about 6.5 nm, 13.3 nm and 10.1 nm respectively, which leads to high quality factor (Q) of 132.9, 74.1 and 109.1 ($Q=\lambda/\Delta\lambda$). The absorption can reach 98.5%, 84.0% and 99.0% achieving tunable narrow-band perfect absorption.

In order to clarify the physical mechanism of narrowband perfect absorption, the relative electric $|E|^2$ and magnetic field $|H|^2$ distributions at the wavelengths of triple absorption peaks A_1, A_2 and A_3 are simulated on the X-Z plane when the radius r is 160 nm and period L is 700 nm as the Fig. 3 shown. As we can see, for the absorption peak A_1, when the wavelength is 864.0 nm, the electric fields are concentrated into the Si layer due to the nature of electric dipole (ED) resonance. In contrast, for the absorption peak A_2, when the wavelength is 985.0 nm, the magnetic fields are concentrated into the Si layer which exhibits the nature of magnetic dipole (MD) resonance. While for the absorption peak A_3, at the wavelength of 1102.0 nm, the electric

Optics EXPRESS

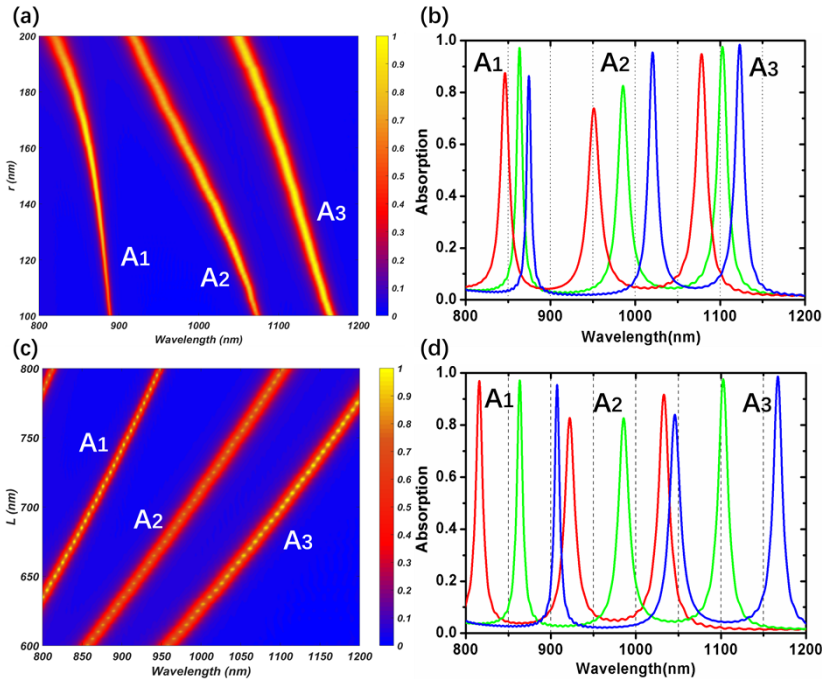

Fig. 2. (a) Simulated absorption for the proposed structure as a function of wavelength and the different radius of the hole r with fixed period $L = 700$ nm. (b) Red, green and blue lines indicate simulated absorption for three radiuses of 140 nm, 160 nm and 180 nm with fixed period $L = 700$ nm. (c) Simulated absorption for the proposed structure as a function of wavelength and the period of the hole L with fixed radius $r = 160$ nm. (d) Red, green and blue lines indicate simulated absorption for three period of 650 nm, 700 nm and 750 nm with fixed radius $r = 160$ nm.

fields and magnetic fields are mainly localized in the middle SiO_2 layer between the Ag and Si layers, which exhibits the nature of plasmonic resonance. In the proposed triple layer structure, the metal Ag with a large imaginary part of refractive index has high absorption characteristic, while for the material Si, the imaginary part of refractive index is relatively small with a weak absorption characteristic. When the electromagnetic resonance modes supported by the proposed structure occur, these absorbent materials can consume the incident light of resonant wavelengths, which leads to perfect absorption.

Furthermore, the absorption distributions of the proposed triple layers can be calculated directly by the Ohmic loss equation [48]:

$$\mathrm{Q}(r, w) \;=\; \frac{1}{2} \times w \times \;\mathrm{Im}\,(\varepsilon)\;. \times E(r, w)^2 \tag{1}$$

in which Im(ε) is the imaginary part of the dielectric permittivity, w is the angular frequency, and E (r, w) is the electric field intensity extracted from the FDTD simulation results in Fig. 3, therefore the Ohmic loss Q (r, w) calculated by Eq. (1) is not the true value but the relative distributions. Figure 4 shows the calculated results for the absorption peak A_1, A_2 and A_3 when the period and radius of the nano hole array are 700 nm and 160 nm respectively. The imaginary part of dielectric constant for Ag, SiO_2, and Si material extracted from Palik data are used in the calculation at the resonant absorption peaks 864.0 nm, 985.0 nm, and 1102.0 nm. As we can see in Fig. 4(a), the Ohmic loss mainly generates in Si layer because this electromagnetic mode caused by ED resonance, the electric fields are concentrated into the Si layer. While in Fig. 4(b)

Optics EXPRESS

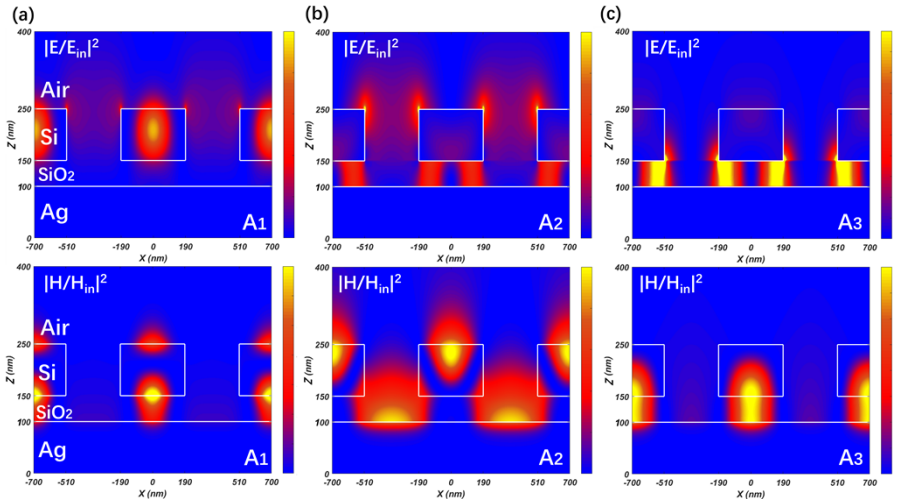

Fig. 3. (a), (b) and (c) The relative electric field and magnetic field intensity distributions at the absorption peaks A_1, A_2 and A_3. The period and radius of the hole array are $L = 700$ nm, $r = 160$ nm for the proposed triple layer structure.

and Fig. 4(c) the Ohmic loss mainly generates in the underlying Ag film, because the electric fields mainly concentrate and form resonance in the middle SiO_2 layer. At this moment, the Ohmic loss distribution in Si layer is very little due to the reduced imaginary part of the dielectric permittivity of Si from short wave to long wave. This part of the content also indicates that the physical mechanism of perfect absorption for the proposed tripe layer structure is the Ohmic loss caused by the metal Ag and weak absorbent semiconductor Si.

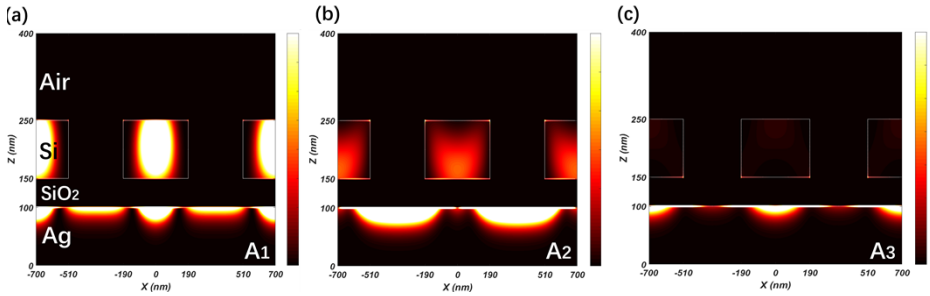

Fig. 4. Ohmic loss distributions calculated by Eq. (1) when period is 700 nm, radius is 160 nm. (a), (b), (c) represent the peak A_1, A_2, and A_3, respectively.

4. Experimental validation

The nano hole array in this work is fabricated by the self-assembled nanosphere lithography [49–53], the fabrication process is shown in the Fig. 5. Firstly, Ag and SiO_2 film with thickness of 100 nm and 50 nm were coated on the glass substrate in sequence. Then closely packed monolayer PS nanospheres with diameter of 700 nm were obtained on water-air interfaces by self-assembly method. The final size of the PS nanospheres were decreased by oxygen plasma using reactive ion etching (RIE) in a controlled manner. Therefore, we can obtain the size of the microspheres as we want by controlling the etching time. Afterward, 100 nm thick Si layer was deposited vertically on the non-close packed PS sphere mask. After removing these PS spheres,

Optics EXPRESS

nanohole array can be formed in the top Si layer. It should be noted that the period of the nano hole array can be adjusted by changing the diameter of the PS nanosphere, while for the diameter of the nano holes can be controlled by different etching time in RIE procedure. The magnetron sputtering method was used to fabricate the Ag, SiO_2, and Si thin film. The sputter target was purchased from ZhongNuo Advanced Material (Beijing) Technology Co., Ltd.

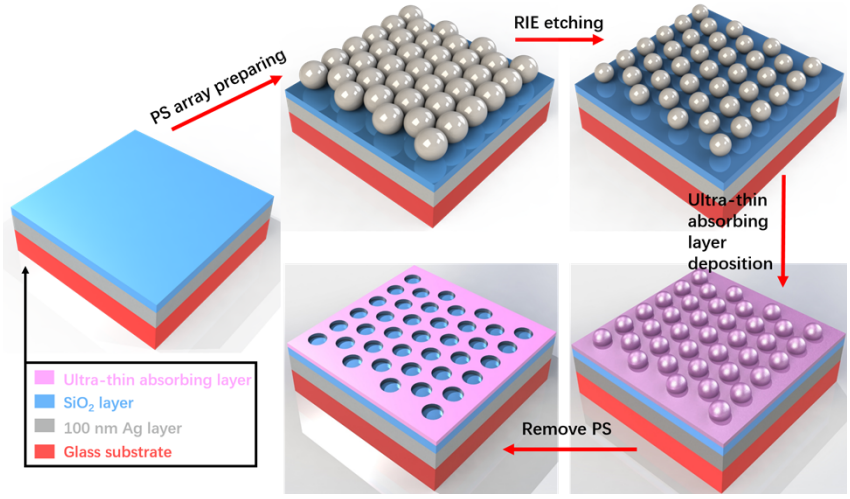

Fig. 5. Fabrication process flow of the proposed triple layer with nano-hole array in the top Si layer.

Figure 6(a) and 6(b) shows the top-view scanning electron microscopy (SEM) images of the PS sphere (700 nm diameter) monolayer. As we can see the PS nanospheres are clear and aligned. After oxygen plasma etching, the size of the PS nanospheres are reduced significantly as the Fig. 6(c) shown. Figure 6(d) is the SEM image of the ultimate nano hole array with the period of 700 nm and hole radius of 160 nm, which is in a hexagonal lattice displaying a high-quality order.

The experimental reflection is measured by PE Lambda 1050 with a 150 mm integrating sphere. A plate with a 1 mm circular hole in diameter was placed before the sample. The measuring range is set from 800 nm to 1200 nm with a fixed interval of 0.2 nm. And the experimental absorption spectrum indicated by the red line in the Fig. 7 is calculated by the equation of A = 1-R. As we can see, three narrow absorption peaks A_1, A_2 and A_3 with narrow band occur at the wavelength of 874.0 nm, 983.0 nm and 1125.0 nm respectively. The FWHM of the three absorption peaks are 12.2 nm, 10.1 nm and 21.5 nm. The maximum absorption is 98.3%, 76.1% and 97.2%. The simulated absorption by FDTD method is shown as the green line in Fig. 7. The experimental and simulation results are in good agreement, which proves the correctness of the simulation. Comparison of the results are shown in Table 1. It should be noted that the nano-hole array fabricated by the nanosphere lithography is not a standard cylinder and the radius of the nano hole cannot be obtained accurately and also the permittivity of Ag, Si and SiO_2 used in simulation is different from the experiment, which result in some deviation between the experimental and simulated results. Furthermore, the performance of proposed triple layer absorber was compared to some previously published papers, such as Refs. [42–46], most of which stayed in theoretical simulation without any experiment. Therefore, the behavior of our proposed absorber is considerably better.

Optics EXPRESS

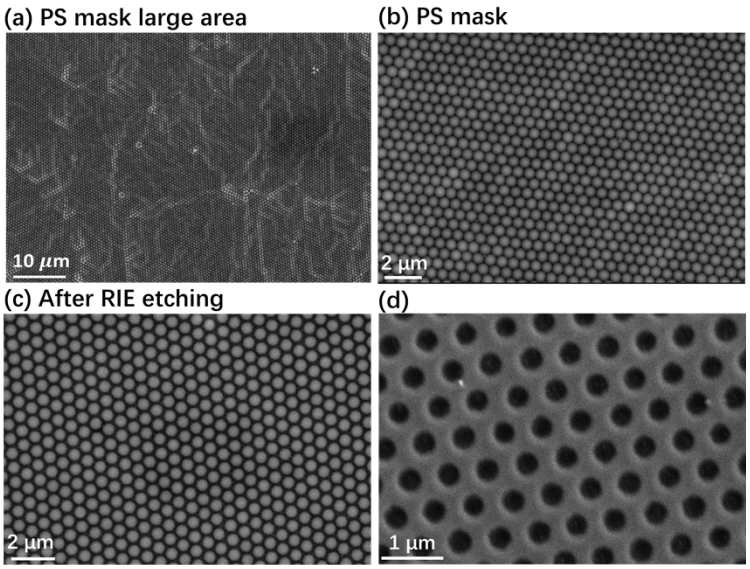

Fig. 6. (a) (b) A large area of the close packed PS monolayer template. (c) Non-closed PS sphere monolayer after oxygen plasma etching. (d) The top view of sample with the period 700 nm and radius 160 nm.

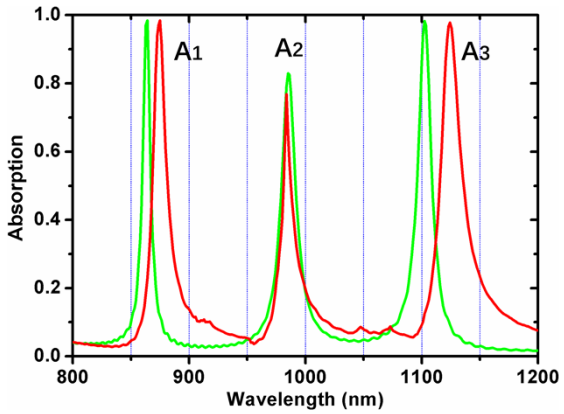

Fig. 7. Simulated (green line) and experimental (red line) absorption of the proposed triple layer structure with the period $L = 700$ nm and $r = 160$ nm.

Table 1. The simulated and experimental results

	Simulated results by FDTD			Experimental results		
	A_1	A_2	A_3	A_1	A_2	A_3
Wavelength(nm)	864.0	985.0	1102.0	874.0	983.0	1125.0
Max absorption (%)	98.5	84.0	99.0	98.3	76.1	97.2
FWHM (nm)	6.5	13.3	10.1	12.2	10.1	21.5
Quality factor Q	132.9	74.1	109.1	71.6	98.4	52.3

Optics EXPRESS

5. Conclusion

In conclusion, we have successfully demonstrated a triple layer consisting of the bottom Ag layer, thin SiO_2 space layer, and ultrathin semiconductor Si film with nano hole array achieving three absorption peaks with narrow band. We also clarified the physical mechanism of the proposed structure in details by FDTD simulation, in which the three narrow band perfect adsorption peaks can be attributed to ED resonance, MD resonance and plasmonic resonance respectively. At the same time, we used a low-cost nanosphere lithography method to fabricate the proposed nano hole array in large area. By characterizing and measuring the fabricated structure, the absorption peak can reach up to 98.3% and the narrowest FWHM can reach up to 10.1 nm in experiment. The highest quality factor Q can reach up to 98.4. The simulated and experimental results fit each other well which further demonstrates the correctness of the work. This work can open a new avenue for narrow band perfect absorption using ultrathin semiconductor film and benefit for many fields such as infrared sensors, plasmonic filters, and hyperspectral imaging.

Funding. National Natural Science Foundation of China (12204478, 61905238).

Disclosures. The authors declare no conflicts of interest.

Data availability. Data underlying the results presented in this paper are not publicly available at this time but may be obtained from the authors upon reasonable request.

References

1. C. M. Watts, X. L. Liu, and W. J. Padilla, "Metamaterial electromagnetic wave absorbers," Adv. Mater. **24**, 98–120 (2012).
2. C. F. Guo, T. S. Sun, F. Cao, Q. Liu, and Z. F. Ren, "Metallic nanostructures for light trapping in energy-harvesting devices," Light: Sci. Appl. **3**, e161 (2014).
3. Q. Li, J. S. Gao, H. G. Yang, and H. Liu, "A super meta-cone absorber for near-infrared wavelengths," Plasmonics **11**(4), 1067–1072 (2016).
4. Y. Zhou, T. Qin, Z. Z. Liang, D. J. Meng, X. Y. Xu, D. R. Smith, and Y. C. Liu, "Ultra-broadband metamaterial absorbers from long to very long infrared regime," Light: Sci. Appl. **10**(1), 138 (2021).
5. A. Nagarajan, K. Vivek, M. Shah, V. G. Achanta, and G. Gerini, "A broadband plasmonic metasurface superabsorber at optical frequencies: analytical design framework and demonstration," Adv. Opt. Mater. **6**(16), 1800253 (2018).
6. B. Park, S. H. Yun, C. Y. Cho, Y. C. Kim, J. C. Shin, H. G. Jeon, Y. H. Huh, I. Hwang, K. Y. Baik, Y. I. Lee, H. S. Uhm, G. S. Cho, and E. H. Choi, "Surface plasmon excitation in semitransparent inverted polymer photovoltaic devices and their applications as label-free optical sensors," Light: Sci. Appl. **3**(12), e222 (2014).
7. Z. D. Yong, S. L. Zhang, C. S. Gong, and S. L. He, "Narrow band perfect absorber for maximum localized magnetic and electric field enhancement and sensing applications," Sci. Rep. **6**(1), 24063 (2016).
8. T. Allsop, R. Arif, R. Neal, K. Kalli, V. Kundrát, A. Rozhin, P. Culverhouse, and D. J. Webb, "Photonic gas sensors exploiting directly the optical properties of hybrid carbon nanotube localized surface plasmon structures," Light: Sci. Appl. **5**(2), e16036 (2016).
9. B. D. Dana, J. Boyu, J. Q. Lin, L. N. Li, A. N. Koya, and W. Li, "Hybrid plasmonic modes for enhanced refractive index sensing," Adv. Sensor Res. **8**, 2300066 (2023).
10. S. Khani and M. Hayati, "Optical sensing in single-mode filters base on surface plasmon H-shaped cavities," Opt. Commun. **505**, 127534 (2022).
11. M. R. Rakhshani, "Narrowband plasmonic absorber using gold nanoparticle arrays for refractive index sensing," IEEE Sens. J. **22**(5), 4043–4050 (2022).
12. M. R. Rakhshani and M. A. Mansouri-Birjandi, "High-sensitivity plasmonic sensor based on metal–insulator–metal waveguide and hexagonal-ring cavity," IEEE Sens. J. **16**(9), 3041–3046 (2016).
13. H. Chalabi, D. Schoen, and M. L. Brongersma, "Hot-electron photodetection with a plasmonic nanostripe antenna," Nano Lett. **14**(3), 1374–1380 (2014).
14. H. Ding, S. L. Wu, C. Zhang, L. J. Li, Q. X. Sun, L. W. Zhou, and X. F. Li, "Tunable infrared hot-electron photodetection by exciting gap-mode plasmons with wafer-scale gold nanohole arrays," Opt. Express **28**(5), 6511–6520 (2020).
15. B. Y. Zheng, Y. M. Wang, P. Nordlander, and N. J. Halas, "Color-selective and CMOS-compatible photodetection based on aluminum plasmonics," Adv. Mater. **26**(36), 6318–6323 (2014).
16. Y. Z. Chu, M. G. Banaee, and K. B. Crozier, "Double-resonance plasmon substrates for surface-enhanced raman scattering with enhancement at excitation and stokes frequencies," ACS Nano **4**(5), 2804–2810 (2010).
17. G. L. Liu, Y. Lu, J. Kim, J. C. Doll, and L. P. Lee, "Magnetic nanocrescents as controllable surface-enhanced raman scattering nanoprobes for biomolecular imaging," Adv. Mater. **17**(22), 2683–2688 (2005).
18. M. Zamuner, D. Talaga, F. Deiss, V. Guieu, A. Kuhn, P. Ugo, and N. Sojic, "Fabrication of a macroporous microwell array for surface-enhanced raman Scattering," Adv. Funct. Mater. **19**(19), 3129–3135 (2009).

Optics EXPRESS

19. C. An, S. Peng, and Y. G. Sun, "Facile synthesis of sunlight-driven AgCl-Ag plasmonic nanophotocatalyst," Adv. Mater. **22**(23), 2570–2574 (2010).
20. F. Pincella, K. Isozaki, and K. Miki, "A visible light-driven plasmonic photocatalyst," Light: Sci. Appl. **3**(1), e133 (2014).
21. S. Thangudu, S. S. Kulkarni, R. Vankayala, C. S. Chiang, and K. C. Hwang, "Photosensitized reactive chlorine species-mediated therapeutic destruction of drug-resistant bacteria using plasmonic core–shell Ag@AgCl nanocubes as an external nanomedicine," Nanoscale **12**(24), 12970–12984 (2020).
22. Q. Li, J. S. Gao, H. G. Yang, H. Liu, X. Y. Wang, Z. Z. Li, and X. Guo, "Tunable plasmonic absorber based on propagating and localized surface plasmons using metal-dielectric-metal structure," Plasmonics **12**(4), 1037–1043 (2017).
23. Q. Li, Z. Z. Li, H. G. Yang, H. Liu, X. Y. Wang, J. S. Gao, and J. L. Zhao, "Novel aluminum plasmonic absorber enhanced by extraordinary optical transmission," Opt. Express **24**(22), 25885–25893 (2016).
24. Y. R. Qu, Q. Li, H. Gong, K. K. Du, S. G. Bai, D. Zhao, H. Ye, and M. Qiu, "Spatially and spectrally resolved narrowband optical absorber based on 2D grating nanostructures on metallic films," Adv. Opt. Mater. **4**(3), 488 (2016).
25. Q. Li, Z. Z. Li, X. Y. Wang, T. T. Wang, H. Liu, H.G. Yang, Y. Gong, and J. S. Gao, "Structurally tunable plasmonic absorption bands in a self-assembled nano-hole array," Nanoscale **10**(40), 19117–19124 (2018).
26. J. B. Gao, J. S. Gao, H. G. Yang, H. Liu, X. Y. Wang, K. Wang, X. Y. Liu, Q. Li, Y. C. Wang, Z. Z. Li, R. Q. Gao, and Z. Zhang, "Cavity-driven hybrid plasmonic ultra-narrow bandpass filter," Opt. Express **27**(15), 20397–20411 (2019).
27. M. R. Rakhshani and M. Rashki, "Metamaterial perfect absorber using elliptical nanoparticles in a multilayer metasurface structure with polarization independence," Opt. Express **30**(7), 10387–10399 (2022).
28. L. Yu, Y. Z. Liang, H. X. Gao, K. L. Kuang, Q. Wang, and W. Peng, "Multi-resonant absorptions in asymmetric step-shaped plasmonic metamaterials for versatile sensing application scenarios," Opt. Express **30**(2), 2006–2017 (2022).
29. Z. Qin, X. Y. Shi, F. M. Yang, E. Z. Hou, D. J. Meng, C. F. Sun, R. Dai, S. T. Zhang, H. Liu, H. Y. Xu, and Z. Z. Liang, "Multi-mode plasmonic resonance broadband LWIR metamaterial absorber based on lossy metal ring," Opt. Express **30**(1), 473–483 (2022).
30. T. Sannomiya, H. Saito, J. L Junesch, and N. Yamamoto, "Coupling of plasmonic nanopore pairs: facing dipoles attract each other," Light: Sci. Appl. **5**(9), e16146 (2016).
31. J. W. Nelson, G. R. Knefelkamp, A. G. Brolo, and N. C. Lindquist, "Digital plasmonic holography," Light: Sci. Appl. **7**(1), 52 (2018).
32. Z. Y. Li, S. Butun, and K. Aydin, "Ultranarrow band absorbers based on surface lattice resonances in nanostructured metal surfaces," ACS Nano **8**(8), 8242–8248 (2014).
33. X. L. Hu, L. B. Sun, B. B. Zeng, L. S. Wang, Z. G. Yu, S. A. Bai, S. M. Yang, L. X. Zhao, Q. L. M. Qiu, R. Z. Tai, H. J. Fecht, J. Z. Jiang, and D. X. Zhang, "Polarization-independent plasmonic subtractive color filtering in ultrathin Ag nanodisks with high transmission," Appl. Opt. **55**(1), 148–152 (2016).
34. M. A. Kats, R. Blanchard, P. Genevet, and F. Capasso, "Nanometre optical coatings based on strong interference effects in highly absorbing media," Nat. Mater. **12**(1), 20–24 (2013).
35. J. Y. Lu, S. H. Nam, K. Wilke, A. Raza, Y. E. Lee, A. Alghaferi, N. X. Fang, and T. J. Zhang, "Localized surface plasmon-enhanced ultrathin film broadband nanoporous absorbers," Adv. Opt. Mater. **4**(8), 1255–1264 (2016).
36. T. gong and J. N. Munday, "Near-perfect (>99%) dual-band absorption in the visible using ultrathin semiconducting gratings," Opt. Express **30**(20), 36500–36508 (2022).
37. K. Lee, J. Y. Jang, S. J. Park, C. G. Ji, S. M. Yang, L. J. Guo, and H. J. Park, "Angle-insensitive and CMOS-compatible subwavelength color printing," Adv. Opt. Mater. **4**(11), 1696–1702 (2016).
38. D. Liu, L. Wang, Q. Y. Cui, and L. J. Guo, "Planar metasurfaces enable high-efficiency colored perovskite solar cells," Adv. Sci. **5**(10), 1800836 (2018).
39. I. Staude, A. E. Miroshnichenko, M. Decker, N. T. Fofang, S. Liu, E. Gonzales, J. Dominguez, T. S. Luk, D. N. Neshev, I. Brener, and Y. Kivshar, "Tailoring directional scattering through magnetic and electric resonances in subwavelength silicon nanodisks," ACS Nano **7**(9), 7824–7832 (2013).
40. P. Moitra, B. A. Slovick, W. Li, I. I. Kraavchencko, D. P. Briggs, S. Krishnamurthy, and J. Valentine, "Large-scale all-dielectric metamaterial perfect reflectors," ACS Photonics **2**(6), 692–698 (2015).
41. P. Molet, J. L. Garcia-Pomar, C. Matricardi, M. Garriga, M. I. Alonso, and A. Mihi, "Ultrathin semiconductor superabsorbers from the visible to the near-infrared," Adv. Mater. **30**(9), 1705876 (2018).
42. B. C. P. Sturmberg, T. K. Chong, D. Y. Choi, T. P. White, L. C. Botten, K. B. Dossou, C. G. Poulton, K. R. Catchpole, R. C. McPhedran, and C. M. D. Sterke, "Total absorption of visible light in ultrathin weakly absorbing semiconductor gratings," Optica **3**(6), 556–562 (2016).
43. Y. L. Liao and Y. Zhao, "An ultra-narrowband absorber with a dielectric-dielectric-metal structure based on guide-mode resonance," Opt. Commun. **382**, 307–310 (2017).
44. M. Qin, S. X. Xia, X. Zhai, Y. Huang, L. L. Wang, and L. Liao, "Surface enhanced perfect absorption in metamaterials with periodic dielectric nanostrips on silver film," Opt. Express **26**(23), 30873–30881 (2018).
45. F. Wu, C. F. Fan, K. J. Zhu, J. J. Wu, X. Qi, Y. Sun, S. Y. Xiao, H. T. Jiang, and H. Chen, "Tailoring electromagnetic responses in a coupled-grating system with combined modulation of near-field and far-field couplings," Phys. Rev. B **105**(24), 245417 (2022).

Optics EXPRESS

46. K. Moriasa, H. Hasebe, and H. Sugimoto, "Bound states in the continuum (BIC) in silicon nanodisk array on mirror structure: perfect absorption associated with quasi-BIC below the bandgap," J. Appl. Phys. **133**(17), 173102 (2023).
47. E. D. Palik, *Handbook of Optical Constants of Solids* (Academic, 1985).
48. J. M. Hao, L. Zhou, and M. Qiu, "Nearly total absorption of light and heat generation by plasmonic metamaterials," Phys. Rev. B **83**(16), 165107 (2011).
49. H. Park, D. Shin, G. Kang, S. Baek, K. Kim, and W. J. Padilla, "Broadband optical antireflection enhancement by integrating antireflective nanoislands with silicon nanoconical-frustum arrays," Adv. Mater. **23**(48), 5796–5800 (2011).
50. N. Vogel, L. D. Viguerie, U. Jonas, C. K. Weiss, and K. Landfester, "Wafer-scale fabrication of ordered binary colloidal monolayers with adjustable stoichiometries," Adv. Funct. Mater. **21**(16), 3064–3073 (2011).
51. B. J. Zhang, Y. F. Li, X. M. Zhang, and B. Yang, "Colloidal self-assembly meets nanofabrication: from two-dimensional colloidal crystals to nanostructure arrays," Adv. Mater. **22**(38), 4249–4269 (2010).
52. J. Yu, Q. F. Yan, and D. Z. Shen, "Co-self-assembly of binary colloidal crystals at the air-water interface," ACS Appl. Mater. Interfaces **2**(7), 1922–1926 (2010).
53. S. H. Lee, K. C. Bantz, N. C. Lindquist, S. H. Oh, and C. L. Haynes, "Self-assembled plasmonic nanohole arrays," Langmuir **25**(23), 13685–13693 (2009).